Thermal imaging at plant level to assess the crop-water status in almond trees (*cv.* Guara) under deficit irrigation strategies

García-Tejero I.F.[1]*, Rubio, A.E[2]., Viñuela, I[1]., Hernández, A[1]., Gutiérrez-Gordillo, S[1]., Rodríguez-Pleguezuelo, C.R.[3], Durán-Zuazo V.H.[3]

[1] Instituto Andaluz de Investigación y Formación Agraria, Pesquera y de la Producción Ecológica (IFAPA). Centro "Las Torres – Tomejil". Ctra. Sevilla-Cazalla Km. 12,2. 41.200. Alcalá del Río, Sevilla, Spain.

[2] Facultad de Biología. Departamento de Biología Vegetal y Ecología. Universidad de Sevilla. Avenida de Reina Mercedes s/n. 41012. Sevilla, Spain.

[3] Instituto Andaluz de Investigación y Formación Agraria, Pesquera y de la Producción Ecológica (IFAPA). Centro "Camino de Purchil". Apdo. 2027, 18080, Granada, Spain

*e-mail: ivanf.garcia@juntadeandalucia.es

Abstract

Almond (*Prunnus dulcis* Mill.) has been traditionally associated to marginal land cultivation and rain-fed agriculture in South Spain. However, in the last years, this crop is being progressively introduced in more productive agricultural areas within the Guadalquivir river basin, where the available water resources are not enough to satisfy the adequate crop-water requirements. Considering this limitation, a more precise irrigation scheduling to maximize the yield is required. Infrared thermal imaging emerges as alternative to other traditional methodologies to assess the crop-water status, especially when deficit irrigation (DI) strategies are being applied. The aim of this study was to define the methodology to assess the almond water status by means of thermal information. The trial was conducted during 2014, during the kernel-filling period, in an almond experimental orchard (SW Spain), with 5-year-old trees, subjected to three irrigation regimes: i) a full-irrigation treatment (C-100), which received 100% of ET_C; ii) a regulated deficit irrigation (RDI-50), which received 100% of ET_C except during the kernel filling period, when this treatment was irrigated with 50% of ET_C; iii) and a low-frequency deficit irrigation treatment (LFDI), which received 100% of ET_C except during the kernel filling period, when it was subjected to continuous periods of irrigation-restriction, defined in terms of the threshold values of shaded leaf water potential (Ψ_{leaf}). Three daily curves of canopy temperature (T_C), stomatal conductance to water vapour (g_s) and Ψ_{leaf} with measurements at 8:00, 11:00, 14:00, 17:00 and 20:00 were developed. Additionally, Crop Water Stress Index (*CWSI*), temperature difference between canopy and the surrounding air ($\Delta T_{canopy\text{-}air}$), and the relative index to stomatal conductance (I_G) obtained at different scales (canopy and row) were estimated. Significant correlations of infrared thermal information *vs.* Ψ_{leaf} and g_s were obtained ($p \leq 0.05$ and $p \leq 0.01$), in particular, by using the thermal readings taken at 11:30, 14:30 at 17:30 h, especially robust were the relationships obtained between T_C and *CWSI* with Ψ_{leaf} at 11:30 h; and between T_C and *CWSI* with g_s, and Ψ_{leaf} at 14:30 h. Finally, considering the infrared thermal monitoring procedure (readings at tree and row level), similar values of T_C were obtained, and therefore, the images taken at row level offered a better information with a higher feasibility in terms of image processing.

Keywords: Thermography, thermal indexes, water stress, leaf gas exchange and leaf water potential.

1.- Introduction

Irrigated agriculture in the South of Europe, and more concretely in semi-arid areas such as Andalusia (S Spain), is crucial for their development, especially in those rural regions with a lower economic potential. In this line, for the case of Andalusia, irrigated agriculture generates more than 60% of rural employments, and represents 64% of agricultural production. Currently, 1,176,000 ha are devoted to irrigated agriculture, corresponding to 24% of total Andalusian agricultural surface, and this being 33% of the irrigated agriculture in Spain (ARA, 2011).

Climatic conditions in this area are characterized by the scarcity and irregularity of rainfall, coinciding the dry period with the season of highest evapotranspiration. Moreover, the last forecast predictions argue significant water resources depletions; with an important declining in the soil water reserves, more accused periods of rainfall restrictions and increasing in the average temperatures (IPCC, 2014). In this agreement, it is expected that this situation promotes an imbalance between the irrigation demand and the available water resources in the Mediterranean agriculture (Daccache et al. 2012, Olesen et al. 2011). This fact will suppose an important constraint for the competitiveness between agriculture and other more productive sectors such as the industry or tourism. In addition, the introduction of alternative crops in order to maximize the profitability of agroecosystems will be required, together with different strategies to improve the agricultural water management (García-Tejero et al. 2014a).

In this context, almond (*Prunus dulcis* Mill.) is the third crop in terms of surface in Spain, representing globally almost 40%, and 84% within the EU. However, only 5% of the global production is developed in Spain (FAOSTAT, 2016). Concretely, the surface of almond in Andalusia is about 152,000 ha, and within them, 95% are associated to marginal and rain-fed agriculture because of the climate limitations, where annual rainfalls does not exceed of 300 mm with low nut yields (CAPDR, 2016). However, in the last few years, the agricultural surface devoted to almond crop has significant increased, specially, in areas where this crop was not traditionally cultivated, these new orchards being cultivated under intensive and irrigation practices. Thus, almond can be found under very different agricultural systems from the most marginal situations to the most intensive orchards, which promotes a wide range of yields (from 150 to 2,600 kg ha^{-1}) (CAPDR, 2016).

According to Goldhamer and Fereres (2016), irrigation is the most limiting factor for this crop, with crop water-requirements oscillating between 900 and 1,350 mm (Goldhamer and Girona, 2012). In this agreement, Goldhamer and Fereres (2016) reported values close to 4,000 kg ha^{-1} (depending on the cultivar) for irrigation doses around 1,250 mm, with yield reductions close to 14% when the irrigation doses were close to 1,000 mm. More recently, López-López et al. (2018) in a long-term experience developed in the province of Córdoba (Andalusia, South Spain), reported maximum yield values (> 2,500 kg ha^{-1}) in mature almond trees (cv. Guara), when these trees were irrigated receiving the maximum crop water requirements (close to 10,000 m^3 ha^{-1}).

In spite of this, almond is considered a drought-resistant crop because of its xeromorphic properties (Torrecillas et al. 1996), and many authors have reported different results related to the effects of deficit irrigation (DI) strategies (Puerto et al., 2013; Phogat et al., 2013; 2018; Spinelli et al., 2016; among others). More recently, López-López et al. (2018) discussed the effects of water deficits in almond trees in terms of water use, evaluating different deficit irrigation (DI) strategies during three consecutive years. These authors found that almond trees under different moderate DI strategies were able of keeping canopy volumes similar to those trees that were fully irrigated, these being directly related with the almond capability to obtain yield values under moderate deficit irrigation similar to those reported by fully irrigated trees; this fact being accompanied with similar soil water depletions and transpiration level.

Taking into account the maximum crop-water demand, the water scarcity in semi-arid areas, and the proper response of this crop to moderate water stress, DI would be a suitable alternative to reach equilibrium between the available water resources and a proper crop development with final yields able to ensure the competitiveness and feasibility of this crop (García-Tejero et al., 2016a). However, the application of DI strategies requires a proper knowledge about the crop physiological status, with the aim of ensuring the correct crop development without significant compromising the yield and fruit-quality, especially when water-stress is applied in different crop stages (Spinelli et al., 2016). In this sense, according to Puerto et al. (2013), when a DI strategy is applied in fruit trees, this is mainly developed supplying a specific water withholding, taken as reference the crop water requirements by means of the crop evapotranspiration (ET_C), without taking into account the effects of canopy architecture, the degree of canopy cover or the soil management (among others); or without considering the crop physiological status when this water stress is applied. In this regard, the most proper irrigation scheduling should consider the whole of soil-plant-atmosphere system; although in terms or representativeness, the live component (plant) would be offering the most valuable information, inasmuch as this reflects the most integrative information, mainly in terms of final yield.

Traditionally, crop water monitoring has been developed by using punctual measurements of stem (Ψ_{stem}) or leaf (Ψ_{leaf}) water potential at midday or pre-dawn (Ψ_{pd}) (Shackel, 2011; Nortes et al., 2005) or monitoring the gas-exchange parameters such as transpiration (E), stomatal conductance (g_s) or net photosynthetic rate (A) (Gomes-Laranjo et al., 2006).

According to Remorini and Massai (2003), Ψ_{Stem} is not only a proper indicator of plant-water status as well as the crop productivity. In the same vein, Mirás-Avalos et al. (2016) reported that water potential is a suitable indicator of almond water status, although its usefulness is reduced, because of a minimum number of replications are required, and the representativeness in the whole plant is reduced.

In the last years, the use of remote sensing in agriculture, and more concretely, infrared thermal imaging to monitor the crop water status has been progressively introduced (Costa et al., 2013). This technique has been properly described as a good methodology for crop-water monitoring in different woody crops such as citrus (García-Tejero et al., 2011; González-Dugo et al., 2014); young almonds (García-Tejero et al., 2012), vines (García-Tejero et al., 2016b) or olives (Egea et al., 2017). This technique is based on the leaf energy balance. When a water stress situation is applied, plants responds with a partial stomatal closure, reducing the stomatal conductance, limiting the leaf transpiration and promoting an attenuation of the evaporative cooling process, resulting in higher leaf / canopy temperature values (Jones, 1999; 2004).

This technique can be applied at different monitoring scales, from "leaf or canopy" to "orchard or basin" level (Poblete-Echeverría et al., 2014; 2016). The selection of the most proper methodology will be related with the desired goal and the economic availability (Costa et al., 2013). In this sense, the use of thermography at orchard scale by using satellites images, allows to take decisions related to crop variability or irrigation scheduling, but some constraints must be taken into account. On one hand, thermal images taking by satellites have the difficulty of depending of the moment in which the satellite passes above the orchard; and on the other hand, the spatial and spectral resolution is not proper. These constraints could be solved by using of unmanned aerial vehicles (UAVs), despite its economically restrictions. In this sense, the use of thermal images at orchard scale, taken by means of UAVs, requires having the proper technology; and this fact can increase the cost of this tool, becoming less accessible the use of this technology. By the contrast, these sensors can be used at plant level, with thermal cameras much more profitable, easing the accessibility to this technique by the irrigation communities or technicians.

Likewise, the main constraints of this technique are focused in the image processing (many times requiring high time consuming), and the correct interpretation of the infrared thermal information (García-Tejero et al., 2015a). Because of this, many times different relationships between infrared thermal information and other physiological parameters such as g_s, A, E, or Ψ_{stem} are required (Jones 2004; Jones et al., 2009), although these relationships are not always enough robust because of the high dependence of the meteorological conditions (Jones, 1999; 2004), the monitoring proceedings (Costa el al., 2013), the cultivar (Costa et al., 2012; García-Tejero et al., 2016b) or even, the crop phenological stage (Cohen et al., 2015).

Up to day, several authors have developed strategies to optimize this technique, developing different protocols and strategies to take thermal readings under field conditions (Jones et al., 2009; Pou et al., 2014; Poblete-Echeverría et al., 2014, 2016, García-Tejero et al., 2012, 2016b) and describing different relationships between infrared thermal information and physiological parameters.

We hypothesize that thermography could be a suitable technique to monitor almond water status, especially when this is subjected to DI programs. The aim of the present work was to evaluate the performance of thermography under field conditions at two monitoring levels (plant and row) to assess the crop water status in almond trees (*cv*. Guara), determining the best moment of the day to obtain the thermal information and the most robust thermal index to interpret properly the crop-water status.

2. Material and methods

2.1. Experimental site

The trial was conducted during 2014 in an experimental orchard of almonds (*Prunus dulcis* Mill. D.A. Webb *cv*. Guara, grafted onto GF677), located in the Guadalquivir river basin (37º 30' 47'' N; 5º 58' 2'' O) (Seville, SW Spain). Planted in 2009, the trees were spaced 6 x 7 m, and drip irrigated using two pipe lines with emitters of 2.3 L h^{-1}, and 14 emitters per tree. The soil is silty loam, typical Fluvisol (USDA, 2010), 2.5 m deep, fertile, and low inorganic matter content (< 15.0 g kg^{-1}). The roots are located predominately in the first 50 cm of soil, corresponding to the intended wetting depth, although these exceed more than one meter in depth. Soil-water content values at field capacity (–0.033 MPa) and wilting point (–1.5 MPa) were 0.35 and 0.12 m^3 m^{-3} respectively, with an allowable soil-water depletion level of 0.27 m^3 m^{-3}.

The climatology in the study area is attenuated meso-Mediterranean, with an annual ET_0 rate of 1,400 mm and accumulated rainfall of 540 mm, mainly distributed from October to April.

2.2. Irrigation treatments

Three irrigation treatments were applied: i) a full irrigated treatment (C-100), which received 100% of the crop evapotranspiration (ET_c) during the irrigation period (60 – 304 day of the year, DOY), ii) a regulated deficit irrigation (RDI-50), which received 100% of ET_C except during the kernel filling period and pre-harvest; when this treatment was irrigated at 50% of ET_C. According to this, the kernel-filling period took place from 171 to 227 DOY and pre-harvest from 228 to 243 DOY; this period coinciding with the time in which the kernel has finished its growth and the nut split period begins, just before the irrigation withholding (250 DOY) seven days before the harvesting (257 DOY). iii) and a low-frequency deficit irrigation (LFDI) which received the 100% ET_c during the irrigation period, except during the kernel-filling stage and pre-harvest; when this treatment was irrigated according the registered values of Ψ_{leaf} measured in shaded leaves. In this sense, during the kernel-filling period (from 171 to 227 DOY) this treatment was subjected to irrigation-restriction cycles with the following irrigation dynamic: Once started the kernel-filling period, irrigation was supressed, till reaching values of Ψ_{leaf} close to -2.0 MPa. Then, trees were re-watered with the same periodicity and amount of water as C-100 (approximately during 5 - 7 days) till reaching similar values of Ψ_{leaf} to those registered in C-100. Once this threshold value was reached, this treatment was subjected to a new restriction period until the threshold of Ψ_{leaf} (~ -2.0 MPa) was again surpassed. This dynamic of irrigation-restriction cycles was maintained during whole stage of kernel filling period until harvesting.

Irrigation doses were calculated according to the methodology proposed by Allen et al. (1998), obtaining the values of reference evapotranspiration according to the Penman-Monteith equation; by using a weather station installed in the same experimental orchard; and using the crop coefficients obtained by García-Tejero et al. (2015b), which ranged between 0.6 and 1.2. According to this, irrigation doses applied to C-100, RDI-50 and LFDI were 6,850, 4,400 and 4,180 m^3 ha^{-1}, respectively (Table 1).

2.3. Plant measurements

During the experimental period, three daily curves of canopy temperature (T_C), stomatal conductance to water vapour (g_s) and leaf water potential (Ψ_{leaf}) were obtained during the kernel filling and pre-harvest period. These readings were taken at 08:30, 11:30, 14:30, 17:30 and 20:00 h local time, during the days 29th July (Curve 1) (210 DOY); 5th August (Curve 2) (217 DOY) and 27th August (Curve 3) (239 DOY). These days coincided with the irrigation restriction periods of LFDI, with the aim of registering the crop physiological status during periods of maximum water stress in this treatment. In this sense, Curve 2 was developed a week after Curve 1. The reason was that, when Curve 1 was developed, LFDI has been subjected to seven days of irrigation restriction. Taking into account the obtained results during this curve, it was decided to extend this period once more week, in order to register the crop physiological response under a situation of maximum stress. Finally, between Curve 2 and 3, there was a recovery period (from 218 to 225 DOY), being the Curve 3 developed after 14 days without irrigation (in similar conditions at Curve 2).

Table 2 shows the values of air temperature (T_{air}), relative humidity (RH), and vapour pressure deficit (VPD) registered during the sampling days and for each monitoring hour.

Measurements of Ψ_{leaf} were conducted by using a pressure chamber (Soil Moisture Equipment Corp., Sta. Barbara, CA, USA), monitoring 12 trees per irrigation treatment (one leaf per tree), located in the north side of the tree and being totally mature, fresh and shaded, at 1.5 m of height, approximately. Additionally, the stomatal conductance to water vapor (g_s), was measured in these same trees, by using a porometer SC-1 (Decagon Devices, INC, WA, USA), on one leaf completely exposed to the sun per monitored tree, and at 1.5 m of height.

T_C was measured by using a ThermaCam (Flir SC660, Flir Systems, USA, 7-13 μm, 640x480 pixels) throughout the day (8:30h, 11:30h, 14:30h, 17:30h, and 20:00h local time), with emissivity (ε) set at 0.96. Each pixel corresponds to an effective temperature reading (Jones, 2004). Two methodologies were tested to monitor the canopy temperature: i) 12 images were taken at tree level (one image per tree assessed, thee being the same trees in which the measurements of Ψ_{leaf} and g_s were developed), for each daily curve, treatment and moment of the day), and ii) during Curves 1 and 2, thermal images were taken at row level, so that, the trees monitored in the same image were subjected to the same irrigation treatment (Fig. 1).

These images at tree level were taken in the sunlit side of the trees, with the imager placed at 2 m of the canopy (Fig. 1). Background temperature was determined by measuring the temperature of a crumpled sheet of aluminium foil placed close to the leaves of interest using ε= 1 (Jones et al. 2002). To facilitate the further analysis of these images, a cooled white screen was used as background, this being placed behind of each monitored tree to simplify the isolation of the canopy surface through image processing.

Thermal images at tree level were analysed with the software developed by García-Tejero et al. (2012). This software allows to remove those areas or pixels considered stem and the background (Fig. 2).

For the case of the images taken at row level, these were analysed using the software ThermaCam Research Pro (Flir Systems, USA), selecting a specific area on the left and on the right and obtaining the average value of T_C for each area (Fig. 3). This methodology is much faster than the previous described by

García-Tejero et al. (2012), although it does not discriminates the representative areas with the same feasibility, and the areas selection is done according to the visual perspective of the operator.
Considering the T_C values obtained at tree level, three different thermal indicators were calculated: the difference between canopy and the surrounding air ($\Delta T_{canopy\text{-}air}$), the crop water stress index (*CWSI*), and the index of the relative stomatal conductance these being calculated as follows (Costa et al., 2013):

$$\Delta T_{canopy\text{-}air} = T_C - T_{air} \quad (1)$$

$$CWSI = \frac{\Delta T_{canopy-air} - \Delta Twet}{\Delta Tdry - \Delta Twet} \quad (2)$$

$$I_G = \frac{\Delta T_{dry} - \Delta Tcanopy-air}{\Delta Tcanopy-air - \Delta Twet} \quad (3)$$

where $\Delta T_{canopy\text{-}air}$, ΔT_{dry} and ΔT_{wet} are the differences between canopy and air temperature for the crop in the moment of the measurement, when the crop has the stomata fully closed and when it is fully transpiring, respectively. T_C is the canopy temperature and T_{air} the temperature of the surrounding air.

To obtain the reference values of ΔT_{wet}, there was estimated the non-water stress baseline ($\Delta T_{canopy\text{-}air}$ = a + b*VPD) according to Idso et al. (1981), using a ΔT_{dry} value equal to 5 ºC, as it was proposed by Jackson et al. (1981). Non-water stress baseline was estimated using the canopy temperature readings obtained from full irrigated trees (C-100).

2.4. Experimental design and statistical analysis

The experimental design was of randomized blocks, with four replications per irrigation treatment. Each replication had 15 trees (3 rows and 5 trees per row), being monitored the three central rows for each replication (n=12).
For each measurement day, an exploratory descriptive analysis of data (Ψ_{leaf}, g_s and T_C) was conducted by applying a Levene's test to check the variance homogeneity of the studied variables. Significant differences between irrigation treatments ($p \leq 0.05$) in the studied variables were identified by applying a one-way ANOVA and a Tukey's test for treatment separation, with the SPSS statistical software (SPSS Inc., 15.0 Statistical package; Chicago, IL, USA).
To evaluate the non-water stress baselines, a linear correlation analysis was made (n = 15). To evaluate the relationships between variables, a linear correlation analysis between the values of thermal indicators (T_C, $\Delta T_{canopy\text{-}air}$, *CWSI* and I_G) and the crop physiological variables (Ψ_{leaf} and g_s) was made, by using the average values for each treatment and sampling time (n = 9). The obtained correlation coefficients were

used to identify which would be the best time to carry out T_C readings and the most representative thermal index as a proxy for crop physiology traits.

Finally, comparative study between the T_C readings taken at tree and row level was conducted by means of a linear correlation analysis between these values, using the average values for each treatment and the whole data obtained during the two first daily curves (n=30).

3. Results and discussion

3.1. Daily evolution of crop physiological status

Figure 4 shows the evolution of Ψ_{leaf}, g_s, and T_C measured at tree level during the three daily curves developed during the irrigation period in which the water stress regimes were imposed. On overall, as the climatic conditions along the day became more adverse, Ψ_{leaf} reached more negative values, with a final recovery at the end of the day. By contrast, g_s increased during the first readings until reaching a maximum point in which a significant decrease was observed, this coinciding with the moment of the day in which the climatic conditions were more extreme. After this point a slight recovery of g_s was found with the last measurements of the day. In relation to T_C this variable showed a more dependent trend on the climatic conditions along the day, reaching the maximum values in those moments in which the T_{air} values were the highest. During curves 1 and 2, the lowest values of Ψ_{leaf} were reached at 17:30 h, coinciding with the highest VPD values registered during these days; and with the moments in which the T_C values were maximum. Considering the obtained values for each treatment, no differences were observed at 8:30 h, but these were appearing along the day without observing a total recovery between the DI treatments and C-100 at 20:00 h. It is remarkable that the observed differences in terms of Ψ_{leaf} were higher during the Curve 2, this being associated with the more severe climatic conditions detected and the imposed water restriction period for LFDI in this curve, which had been prolonged for a further seven days, in comparison to Curve 1.

Regarding to g_s, during Curve 1, all the treatments showed a growing tendency, reaching the maximum values at 14:30 h (VPD = 2.61 kPa). However, during the Curve 2, the maximum values were observed at 11:30 h (VPD = 1.82), from which g_s decreased, showing a partial recovering in C-100 at the end of the day. This difference observed for the case of g_s could be associated with the more severe climatic conditions registered during the Curve 2, in comparison to the previous one. Finally, it is noticeable that the depletion in T_C was accompanied with a slight recovery of g_s and the slight recovery of Ψ_{leaf} and g_s during the readings at 20:00 h.

Regarding to the values obtained during the Curve 3, it was obtained three weeks after Curve 2, when climate conditions were similar to those observed in the previous one, and LFDI was subjected to 15 days of irrigation restriction. In this sense, it was observed a similar trend to that detected in Curve 2, with the highest values of g_s observed at 11:30 (VPD = 1.31 kPa), with a significant reduction in all the treatments at 14:30 h, followed by a partial recovery at 17:30 h, and a new descend at the end of the day. This decreasing trend occurred at 14:30 h, being this response associated with a partial stomatal closure, when climatic conditions, specially the VPD values are strongly elevated. Even more, this descend in the values of g_s

promoted that, the readings of Ψ_{leaf} between 11:30 and 14:30 were similar, and the partial recovery of g_s at 17:30 was accompanied with a significant lessen values of Ψ_{leaf}.

Relating to the T_C readings, these were highly determined by the climatic conditions. On overall, T_C readings in the three studied treatments were below to air temperature (T_{air}), except the readings taken at 08:30 and 11:30 h for the Curves 2 and 3. The highest differences in T_C between treatments were detected specially in the readings taken at 11:30, 14:30 and 17:00, although these were not as patent as for the case of Ψ_{leaf}.

On overall, and taking into account the monitored physiological variables, it can be assumed that Ψ_{leaf} was the parameter that reflected the highest differences between treatments. In this sense, during the Curve 1, significant differences were observed between C-100 and the remaining treatments at 11:30 and 14:30 h, with an abrupt descend in the readings conducted at 17:30 (<-2.0 MPa), without differences between the three irrigation treatments. During the Curve 2, the Ψ_{leaf} values registered in C-100 were significant different than those registered in the remaining treatments during all day (except at 8:30 h), not being reached the threshold value of -1.5 MPa in C-100. Finally, it also draws attention that, during Curve 3, C-100 reached again Ψ_{leaf} values close to -2.0 MPa, as it was fitted for the Curve 1.

It is remarkable that, whereas Ψ_{leaf} was able to show significant differences between treatments, this fact was not as patent in terms of g_s, because of the low capacity of almond to regulate the stomatal closure under drought conditions. In this regard, almond trees present a fast recovery of water potential, but a delay in the values of g_s as it has been stated by authors such as Torrecillas et al. (1996) or Romero et al. (2004). In this line, in physiological terms, when almond is subjected to a mild-to-moderate water stress situation a stomatal conductance reduction is not as patent as the effects in terms of water potential because of its low capability of regulating the stomata when a water stress situation is applied, as it has been discussed by some authors such as Wartinguer et al. (1990), Egea et al. (2011) or Eichi (2013). In this agreement, previously to observe a significant reduction in g_s, almond responds with significant descends in terms of leaf or stem water potential, (García-Tejero et al, 2012, 2015b). Consequently, almond would be able to maintain acceptable levels of g_s (promoting significant descends in the crop-water potential) but, keeping optimum values of carbon assimilation, photosynthetic rate, and hence increasing the intrinsic water-use efficiency (McCutchan and Shackel, 1992; Rouhi et al., 2007).

Gomes-Laranjo et al. (2006) reported values of Ψ_{leaf} for different cultivars, which ranged between -1.72 and -2.0 MPa in Glorieta; -1.71 and -2.40 MPa in Ferragnes; -1.91 and -2.34 MPa in Francoli; -1.97 and -2.26 MPa in Lauranne, and -1.88 and -1.92 MPa in Masbovera. In this line, these values correspond to measurements done at midday in well-watered trees, which are in line with the threshold range between -1.5 and -2.0 MPa considered and obtained in this work for C-100.

Obviously, this water potential depletion affects to leaf gas exchange. In this sense, for full irrigated conditions, daily cycle of gas exchange is almost constant when no radiation limitation occur (Torrecillas et al., 1988; Klein et al., 2001; Romero et al., 2006) and vapour pressure deficit (VPD) is not higher than 2 KPa (Romero et al., 2006). However, in our case, the values of VPD were higher than this value during the three curves when the readings were taken between 11:30 and 20:00 h, which would explain the daily variation of g_s in this study. Nevertheless, Torrecillas et al. (1988) reported partial stomata closure in the daily cycle this being higher at midday than in the morning (Klein et al 2001) and reduce the sensibility to evaporative demand (Romero et al., 2006).

Regarding to the recovery capability of the DI treatments, the most noticeable was the absence of differences between treatments at the beginning of the day (8:30 h), these values being around -0.5 MPa. That is, although during the day the crop was subjected to water stress conditions, this showed an optimum recovery capacity during the evening and night, although this fact occurred faster in C-100 (as was observed in the readings taking at 20:00 h). This fact could be related to the experimental orchard location, very close to the Guadalquivir river course (~ 100 m). This would explain this certain capability of recovering, being the trees able to take water during the night from deeper soil layers.

3.2. Relationships between thermal parameters and physiological variables

With the aim of stablishing the most appropriate moment to take the thermal readings and the best thermal indicator in order to determine the plant water status, different relationships were obtained between the thermal parameters and the related physiological variables, these relationships being obtained for each monitoring time.

Previously, the non-water stress baseline was defined, which was calculated using the canopy temperature readings obtained from full irrigated trees, and the values of air temperature and vapour pressure deficit in each monitoring time (Figure 5).

We used the methodology proposed by Idso et al. (1981) and Jackson et al. (1981) to derive non-water stressed baselines from the $\Delta T_{canopy\text{-}air}$ values obtained from the C-100 trees (n = 15) and VPD values registered for each time and monitoring day (Table 2). It was noticeable that if these functions had been defined separately for each curve, the slopes of them (-1.84, -1.88 and -1.85 for Curve 1, 2 and 3, respectively) were very similar. According to Berni et al. (2009), for the case of olive, the slope values could be affected by errors in the estimation of T_C and the measurement of T_{air}, although more interesting conclusion was the one derived from the comparison between the effect of net radiation and wind speed in the interception point, suggesting that the slopes obtained for different non-water stressed baselines estimated from a theorist proposed model by them were very similar to the obtained from empirical information; and the highest variations were observed in the interception point. Similar results were reported by Testi et al. (2008) in pistachio trees, evidencing that daily variations in net radiation resulted in parallel baselines, not being affected the slope of baseline. In our case, the non-water stress baselines obtained independently for each curve showed very similar slopes, focusing the differences in the interception points (1.25, 3.64 and 4.22 for Curves 1, 2 and 3, respectively).

Once defined the non-water stress baseline, the values of *CWSI* and I_G were estimated in order to normalize the T_C readings and to define the most advisable thermal index to assess the almond water status using thermal information.

According to García-Tejero et al. (2016b), there are many variables such as the air temperature, vapour pressure deficit, the radiation level, or its angle of incidence on the leaf surface that will influence decisively on the absolute value of T_C and have to be considered. These indexes normalize the absolute values of temperature, obtaining a second value in which the effects of this set of potentially influential variables are partially minimized (García-Tejero et al., 2015a).

Once the T_C readings were normalized with the air temperature and CWSI I_G calculated, the different relationships with Ψ_{leaf} and g_s were defined for each monitoring time considered in the three daily curves (Table 3). According to the results, the most significant relationships were for the readings taken at 11:30, 14:30 and 17:30 h, although some differences were found depending on the thermal indicator and the physiological parameter considered. Thus, it is remarkable that at 11:30 h, the best relationships were fixed between the thermal information and Ψ_{leaf}, whereas the relationships for g_s were not significant.

Therefore, at 11:30 h T_C as well as *CWSI* showed the most significant relationships. When these relationships were obtained for the readings taken at 14:30 h, T_C and *CWSI* reported the most significant relationships again, and in this case, these were noteworthy as for g_s as for Ψ_{leaf}, evidencing that the measurements taken at 14:30 h would be more representative than those fixed at 11:30 h. The robustness of these relationships decreased for the readings taken at 17:30 and 20:00, being not recommendable the readings during the evening and at the end of the day.

Previous literature showed that infrared thermal imaging can be used to assess the crop water status under field conditions (Jones et al., 2002; Möller et al., 2007; García-Tejero et al., 2016b). However, for a proper management of deficit irrigation strategies it is essential to identify the most appropriate and robust thermal index as well as the best time of the day to perform the infrared thermal readings. In our case, we hypothesized that the most appropriate moment would be in those hours of the day at which the most significant differences in terms of T_C and the physiological traits (Ψ_{leaf} and g_s) were detected. That is, the most significant differences between treatments were detected for the readings taken at 11:30, 14:30 and 17:30 h, and especially in terms of Ψ_{leaf}, coinciding this period of the day with the moments under the highest air evaporative demand. In this context, many authors have demonstrated that the best time of the day to do more robust and physiologically meaningful temperature readings was at midday (González-Dugo et al., 2013; Pou et al., 2014; Bellvert et al, 2014; García-Tejero et al., 2011, 2016b). Our findings show that thermal information was highly correlated with Ψ_{leaf} and g_s at 14:30 h (Table 3), and 11:30 h exclusively for the case of Ψ_{leaf}.

The different indicators studied have advantages and disadvantages that must be taken into account when they are used for water-stress monitoring at field level. Regarding the simplicity and the time consuming aspects, the absolute value of T_C and the $\Delta T_{canopy\text{-}air}$ would be more recommendable because they are easy to calculate. Moreover, these have been successfully used in water stress monitoring of relevant woody crops such as citrus (García-Tejero et al., 2011), almonds (García-Tejero et al. 2012), vines (García-Tejero et al., 2016) or olives (García-Tejero et al., 2017), T_C would not be the best water stress indicator, because of the high variability of this parameter in relation to the weather conditions. In this sense, $\Delta T_{canopy\text{-}air}$ would be more representative, especially if this is used taking the derived information from the non-water stress baselines. The simplicity of this indicator could favour its usage as a preliminary indicator of stress. However, it is necessary to consider that this parameter is more influenced by weather conditions than *CWSI*, and hence, it can have major limitations for remote sensing characterization for crop water status, whereas the *CWSI* would be more robust especially under more variable environmental conditions along the day. In this line, Figure 6 shows the relationships between T_C, $\Delta T_{canopy\text{-}air}$ and *CWSI* with Ψ_{leaf} by using the readings taken at 11:30, 14:30 and 17:30 h. According to this, results showed the higher robustness of *CWSI* in comparison to the absolute values of T_C, being a good thermal indicator to monitor the crop water status and estimate the values of Ψ_{leaf} in almond, when these readings are taken within the range of 11:30 and 17:30 h. Similar results were obtained by Gonzalez-Dugo et al. (2013), when they suggested the advantages of taking the thermal readings at midday in order to find the best results in terms of irrigation scheduling and crop water monitoring; although in their case, thermal readings were taken by means of UAV, this strategy being specially recommended to study the crop variability.

Regarding the range of values obtained for *CWSI*, it is remarkable that, in spite of these values should be within the range of 0-1, in our case, some values were below to 0. This fact could be promoted by two questions: the necessity of stablishing references values of T_{wet} and T_{dry}, or maybe, by the fact of improving the non-water stress baselines functions, by using different equations for different phenological stages, different moments along the day. Similar situations have been reported by other authors such as Egea et al. (2017) or García-Tejero et al. (2017) in olives, when these authors used non-water stress baselines calculated by using thermal data from well irrigated trees, and taking as "reference value" of $T_{dry} = T_{air} + 5$ ºC. These assumptions could promote little deviations of CWSI out of the range of [0 – 1].

3.3. Strategies to assess the canopy temperature: readings at two different levels

Finally, once determined the best moment along the day to assess the almond water status by means of infrared thermal readings and the most robust thermal indexes, two different methodologies were assessed to take the images; the first of them, at tree level, and the other at row level. For this, during the curves 1 and 2, together with the thermal readings taken at tree level, images at row level were taken to monitor the canopy of consecutive trees subjected to the same irrigation strategy. Whereas, the first strategy allows to monitor a representative area of one tree, being processed in order to delete those pixels that does not correspond with the canopy; the second strategy allows to monitor a higher number of trees, but the further discrimination to analyse the images is less precise than the previous one.

Tables 4 and 5 show examples of the images taken under these two procedures at different moments along the days, and the average values of T_C obtained at tree and row level. These measurements were related, with the aim of corroborate if the thermal information obtained at tree level, and requiring an image processing, was similar to those obtained using the images taken at row level (with a processing of images faster than that required when these are taken at tree level). As it can be observed, the relationships were highly significant ($p < 0.01$) and very similar to the function $y = x$, evidencing that the obtained measurements at row level were very similar than those obtained for each monitored tree (Figure 7). These results demonstrate that the procedure of capturing images and their subsequent analysis could be done easier without committing the quality and robustness of the provided information.

Although any crop has a set of inherent characteristics; when we want to use the infrared thermal imaging for monitor the crop-water status, one of the most important characteristic to be taken into account will be the crop morphology. In addition, there are some limitations usually associated with the procedure of capturing and processing data, requiring in many cases the use of complex software, thus reducing the operational and affordability of such these techniques. The aim of these methodologies is to exclude those parts of the tree that not are susceptible of being monitored (branches, trunk, etc.) (García-Tejero et al., 2012). Hand-operated cameras allow taking images of individual plants or portions of them, but during the capturing process different elements (soil, shady areas, sky or portions of adjacent plants) can be reflected, requiring a subsequent time-consuming processing images (García-Tejero et al., 2015a). This difficulty is specially marked in woody crops, with discontinuous canopies and a ground cover less than 100% (Jiménez-Bello et al., 2011). Some authors such as Zarco-Tejada et al. (2009), Wang and Gartung (2010), or García-Tejero et al. (2012) have described different methods to overcome such limitations, although all of them have previously required different images processing, either through editing software and image processing, either through processes of classification of pixels, or through relatively laborious statistical analysis. However, attempting to the obtained results in the present work, the thermal information provided by the images taken at row level was very similar to that reported after processing the images taken at tree level. This fact supposes an important consideration in order to standardize the methodology of this technique when this is going to be used by field operators to assess the crop water status aiming to perform irrigation scheduling.

4.- Conclusions

Considering the aims previously defined in the present work, CWSI would be the most appropriate thermal index to monitor the almond water status. In this sense, the normalization achieved using the CWSI significantly improved the possibility of estimating the values of leaf water status, especially when thermal readings are taken between 11:30 and 17:30 h, these coinciding with daily period of maximum evapotranspirative demand.

On the other hand, considering the different scales to take the thermal readings, the results allow us concluding that the images taken at row level were enough robust to be used to estimate the water status, being the canopy temperature values very similar to those obtained at tree level. Nevertheless, some aspects should be considered in future works such as the estimation of different baselines for the different phenological stages in almond, and the effect of the moment of the day in these types of functions.

Therefore, infrared thermal imaging supposes an alternative tool as a non-invasive technique in modern agriculture, addressing in improvement in the water resources management, irrigation scheduling, and the crop water monitoring. According to the findings of the present work, the infrared approach has a great advantage due to the robustness of the provided information, the versatility of the measurements that are taken, and the feasibility in developing experiments at different scales. Thus, infrared thermography is a suitable technique to monitor the almond water status, especially when this is subjected to deficit irrigation strategies.

Acknowledgements

Part of this work was sponsored by the research project "Integrated management of the cultivation of almond and other nuts (INNOVA-Nuts)" (AVA.AVA201601.18), within the Operational Program FEDER 2014-2020 "Andalusia moves with Europe ". The author I. Garcia-Tejero has a contract co-financed by the Operational Program of the European Social Fund (ESF) 2007-2013 "Andalusia moves with Europe".

References

ARA. 2011. Agenda del Regadío Andaluz, Horizonte 2015, Consejería de Agricultura y Pesca, Junta de Andalucía, 127 pp.

Bellvert, J., Zarco-Tejada, P.J., Fereres, E., Girona, J. 2014. Mapping crop water stress index in a `Pinot-noir´ vineyard: comparing ground measurements with thermal remote sensing imagery from an unmanned aerial vehicle. Precision Agric. J. 15, 361-376.

Berni, J.A.J., Zarco-Tejada, P.J., Sepulcre-Canto, G., Fereres, E., Villalobos, F. 2009. Mapping canopy conductance and CWSI in olive orchards using high resolution thermal remote sensing imagery. Remote Sens. Environ. 113, 2380–2388.

CAPDR. 2016. Caracterización del sector de la almendra en Andalucía. Secretaría General de Agricultura y Alimentación, Consejería de Agricultura, Pesca y Desarrollo Rural. Junta de Andalucía. 34 pp. Available from: http://www.juntadeandalucia.es/agriculturaypesca/observatorio/servlet/FrontController?action=RecordContent&table=12030&element=1654785. [02 January 2017].

Cohen, Y.; Alchanatis, V.; Sela, E.; Saranga, Y.; Cohen, S.; Meron, M.; Bosak, A.; Tsipris, J.; Ostrovsky, V.; Orolov, V.; et al. Crop water status estimation using thermography: Multi-year model development using ground-based thermal images. Precis. Agric. 2015, 16, 311–329.

Costa, J.M., Ortuño, M.F., Lopes, C.M., Chaves, M.M. 2012. Grapevine varieties exhibiting differences in stomatal response to water deficit. Funct. Plant Biol. 39, 179-189.

Costa, J.M., Grant, O.M., Chaves, M.M. 2013. Thermography to explore plant-environment interactions. J. Exp. Bot. 64, 3937-3949.

Daccache, A., Keay, C., Jones, R.J.A., Weatherhead, E.K., Stalham, M.A., Knox, J.W. 2012. Climate change and land suitability for potato production in England and Wales: impacts and adaptation. J. Agric. Sci. 150, 161-177.

Egea, G., Dodd, I.C., González-Real, M.M., Domingo, R., Baile, A. 2011. Partial rootzone drying improves almond tree leaf-level water use efficiency and afternoon water status compared with regulated deficit irrigation. Funct. Plant Biol. 38, 372-385.

Egea, G.; Padilla-Díaz, C.M.; Martínez, J.; Fernández, J.E.; Pérez-Ruiz, M. Assessing a crop water stress index derived from aerial thermal imaging and infrared thermometry in super-high density olive orchards. Agric. Water Manag. 2017, 187, 210–221.

Ecchi, V.R., 2013. Water use efficiency in almonds (Prunnus dulcis (mill)D.A. Web) Phd. Thesis. Schod or agriculture, Food arial wine. Faculty of Science. Univ. Of Adelaide.

FAOSTAT. 2016. Food and Agriculture Organisation of the United Nations. Available at: http://www.fao.org/faostat/en/#data/QC. [03 December 2016].

García-Tejero, I., Durán-Zuazo, V.H., Muriel-Fernández, J.L., Jiménez-Bocanegra, J.A. 2011. Linking canopy temperature and trunk diameter fluctuations with other physiological water status tools for irrigation scheduling in citrus orchards. Funct. Plant Biol. 38, 1-12.

García-Tejero, I., Durán-Zuazo, V.H., Arriaga, J., Hernández, A., Vélez, L.M., Muriel-Fernández, J.L. 2012. Approach to assess infrared thermal imaging of almond trees under water-stress conditions. Fruits, 67, 463-474.

García-Tejero, I.F., Durán-Zuazo, V.H., Muriel-Fernández, J.L. 2014a. Towards sustainable irrigated Mediterranean agriculture: implications for Water conservation in semi-arid environments. Water Int. 39, 635-648.

García-Tejero I, Durán-Zuazo V.H., Muriel-Fernández, J.L. 2015a. Thermal imaging to assess the plant water status in woody crops under arid and semi-arid conditions. In: Ferguson G (ed). Arid and Semi-Arid Environments. Nova Publishers. pp 15-35.

García-Tejero, I.F., Hernández, A., Rodríguez, V.M., Ponce, J.R., Ramos, V., Muriel, J.L., Durán-Zuazo, V.H. 2015b. Estimating almond crop coefficients and physiological response to water stress in semiarid environments (SW Spain). J. Agric. Sci. Tech. 17, 1255–1266.

García-Tejero, I.F., Hernández, A., Durán-Zuazo, V.H., Muriel-Fernández, J.L., Perea, F. 2016a. Hacia una mayor sostenibilidad en la agricultura de regadío de Andalucía Occidental: implicaciones para la conservación del agua en ambientes semiáridos. Tocina Estudios Locales, Revista de Investigación Local, 5, 175-190.

García-Tejero, I.F., Costa, J.M., Egipto, R., Lima, R.S.N., Durán, V.H., Lópes, C., Chaves, M.M. 2016b. Thermal data to monitor crop-water status in irrigated Mediterranean viticulture. Agric. Water Manage. 176, 80-90.

García-Tejero, I., Hernández, A., Padilla-Díaz, C.M., Diaz-Espejo, A., Fernández, J.E. 2017. Assessing plant water status in a hedgerow olive orchard from thermography at plant level. Agric. Water Manage, 188, 50-60.

Goldhamer, D.A., Fereres, E. 2016. Establishing an almond water production function for California using long-term yield response to variable irrigation. *Irrig. Sci.* pp. 1–11. doi:10.1007/s00271-016-0528-2 (on line first).

Goldhamer, D.A., Girona, J. 2012. Crop yield response to water: almond' In: Steduto P, Hsiao TC, Fereres E, Raes D (eds) FAO irrigation and drainage Paper No. 66. Food and Agriculture Organization of the United Nations, Rome, pp 358–373

Gomes-Laranjo, J., Coutinho, J.P., Galhano, V., Cordeiro, V. 2006. Responses of five almond cultivars to irrigation: Photosynthesis and leaf water potential. Agric Water Manage. 83, 261-265.

Gonzalez-Dugo, V., Zarco-Tejada, P., Fereres, E. 2014. Applicability and limitations of using the crop water stress index as an indicator of water deficits in citrus orchards. Agric. For. Meteorol. 198-199, 94-104.

Idso, S.B., Jackson, R.D., Pinter, P.J.J., Reginato, R.J., Hatfield, J.L. 1981. Normalizing the stress degree-day parameter for environmental variability. Agric. Meteorol. 24, 45–55.

IPCC. 2014. Climate change 2014. Impacts, adaptations and vulnerabilities. Part B. Regional aspects. Barros, V & Field CB (eds). Cambridge University Press, 688 pp.

Jackson, R.D., Idso, S.B., Reginato, R.J., Pinter, P.J. 1981. Canopy temperature as a crop water-stress indicator. Water Resources Res. 17, 1133-1138.

Jiménez-Bello, M.A., Ballester, C., Castel, J.R., Intrigliolo, D.S. 2011. Development and validation of an automatic termal imaging process for assessing plant water status. Agric. Water Manage. 98, 1497-1504.

Jones, H.G. 1999. Use of infrared thermometry for estimation of stomatal conductance as a possible aid to irrigation scheduling. Agric. Forest Meteorol. 95, 139-149.

Jones, H.G. 2004. Irrigation scheduling: advantages and pitfalls of plant-based methods. J. Exp. Bot. 55, 2427-2436.

Jones, H.G., Stoll, M., Santos, T., de Sousa, C., Chaves, M.M., Grant, O.M. 2002. Use of infra-red thermography for monitoring stomatal closure in the field: application to the grapevine. J. Exp. Bot. 53, 2249-2260.

Jones H.G., Serraj, R., Loveys, B.R., Xiong, L., Wheaton, A., Price, A.H. 2009. Thermal infrared imaging of crop canopies for the remote diagnosis and quantification of plant responses to water stress in the field. Functional Plant Biology 36, 978–979.

Klein, I, Esparza, G., Weinbaum, S.A., DeJong, T.M. 2001. Effects of irrigation deprivation during the harvest period on leaf persistence and function in mature almond trees. Tree Physiol. 21, 1063-1072.

López-López M., Espadafor, M., Testi, L., Lorite, I.J., Orgaz, F., Fereres, E. 2018. Water use of irrigated almond trees when subjected to water deficits. Agric. Water Manage. 195, 84-93.

Mirás-Avalos, J.M.; Pérez-Sarmiento, F.; Alcobendas, R.; Alarcón, J.J.; Mounzer, O.; Nicolás, E. Using midday stem water potential for scheduling deficit irrigation in mid–late maturing peach trees under Mediterranean conditions. Irrig. Sci. 2016a, 34, 161–173.

McCutchan, H., Shackel, K.A. 1992. Stem-water Potential as a Sensitive Indicator of Water Stress in Prune Trees (Prunus domestica L. cv. French). J. Am. Soc. Hort. Sci. 117, 607–611.

Nortes, P.A., Pérez-Pastor, A., Egea, G., Conejero, W., Domingo, R. 2005. Comparison of changes in stem diameter and water potential values for detecting water stress in young almond trees. Agric. Water Manage. 77, 296–307.

Möller, M., Alchanatis, V., Cohen, Y., Meron, M., Tsipris, J., Naor, A., Ostrovsky, V., ,Sprintsin, M., Cohen, S. 2007. Use of thermal and visible imagery for estimating crop water status of irrigated grapevine. J. Exp. Bot. 58, 827–838.

Olesen, J.E., Trnka, M., Kersebaum, K.C., Skjelvåg, A.O., Seguin, B., Peltonen-Sainio, P., Rossi, F., Kozyra, J., Micale, F. 2011, Impacts and adaptation of European crop production systems to climate change. Europ. J. Agron. 34, 96-112.

Phogat, V., Skewes, M.A., McCarthy, M.G., Cox, J.W., Simunek, J., Petrie, P.R. 2017. Evaluation of crop coefficients, wáter poroductivity and wáter balance components for wine grapes iirrigated at different defiti levels by a sub-surface drip. Agric. Water Manage. 180, 22-34.

Poblete-Echeverría, C., Ortega-Farías, S., Zúñiga, M. 2014. Use of infrared thermography on canopies as indicator of water stress in Arbequina olive orchards. Acta Hort, 1057, 399-404.

Poblete-Echeverría, C., Sepúlveda-Reyes, D., Ortega-Farias, S., Zúñiga, M., Fuentes, S. 2016. PLant wáter stress detection based on aerial and terrestrial infrered thermography: a study case from vineyard and olive orchard. Acta Hort 1112, 141-146

Pou, A., Diago, M.P., Medrano, H., Baluja, J., Tardaguila, J. 2014. Validation of thermal indices for water stress status identification in grapevine. Agric. Water Manage. 134, 60-72.

Puerto, P., Domingo, R., Torres, R., Pérez-Pastor, A., García-Riquelme, M. 2013. Remote management of deficit irrigation in almond trees base on maximum daily trunk shrinkage. Water relations and yield. Agric. Water Manage. 126, 33-45.

Remorini, D., Massai, R. 2003. Comparison of water status indicators for young peach trees. Irrig. Sci. 22, 39-46.

Rouhi, V., Samson, R., Lemeur, R., Van Damme, P. 2007. Photosynthetic gas exchange characteristics in three different almond species during drought stress and subsequent recovery. Environ. Exp. Bot. 59, 117–129.

Romero, P., Botía, P., García, F. 2004. Effects of regulated deficit irrigation under subsurface drip irrigation conditions on vegetative development and yield of mature almond trees. Plant and Soil 260, 169–181.

Romero, P., García, J., Botía, P. 2006. 'Cost–benefit analysis of a regulated deficit-irrigated almond orchard under subsurface drip irrigation conditions in South-eastern Spain', Irrig. Sci. 24, 175–184.

Shackel, K. 2011. A plant-based approach to deficit irrigation in trees and vines. HortSci. 46, 173–177.

Spinelli, G.M., Snyder, R.L., Sanden, B.L., Shackel, K.A. 2016. Water stress causes stomatal closure but does not reduce canopy evapotranspiration in almond. Agric. Water Manage. 168, 11-22.

Testi, L., Goldhamer, D.A., Iniesta, F., Salinas, M. 2008. Crop water stress index is a sensitive water stress indicator in pistachio trees. Irrig. Sci. 26, 395–405.

Torrecillas, A., Ruiz-Sanchez, M.C., del Amor, F., León, A. 1988. Seasonal variations on water relations of Amygdalus communis L. under drip irrigated and non irrigated conditions. Plant and Soil. 106, 215-220.

Torrecillas, A., Alarcón, J.J., Domingo, R., Planes, J., Sánchez-Blanco, M.J. 1996. Strategies for drought resistance in leaves of two almond cultivars. Plant Sci. 118, 135–143.

USDA. 2010. Keys to soil taxonomy (11th Edition). United States Department of Agriculture, Natural Resource Conservation Service, 334 pp.

Wartinger, A., Heilmeier, H., Hartung, W., Schulze, E.D. 1990. Daily and seasonal courses of leaf conductance and abscisic acid in the xylem sap of almond trees (Prunus dulcis (Miller) D.A.Webb) under desert conditions. New Phytol. 116, 581–587.

Zarco-Tejada, P.J., Berni, J.A.J., Suárez, L., sepulcré-Cantó, G., Morales, F., Miller, J.R. 2009. Imaging chlorophyll fluorescence with an airbone narrow-band multispectral camera for vegetation stress detection. Remote Sens. Environ. 113, 1262-1275.

FIGURES

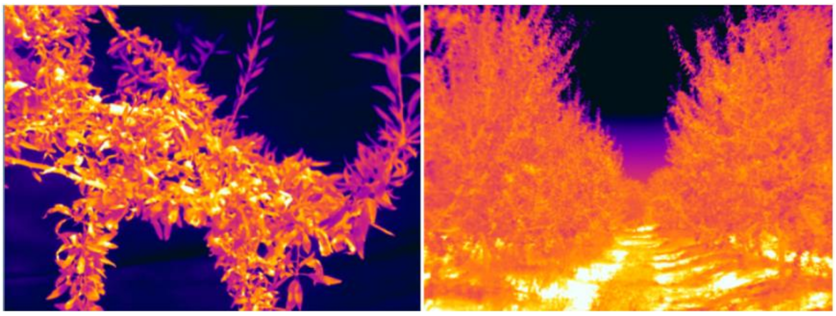

Figure 1. Example of thermal images at plant (left) and row (right) level

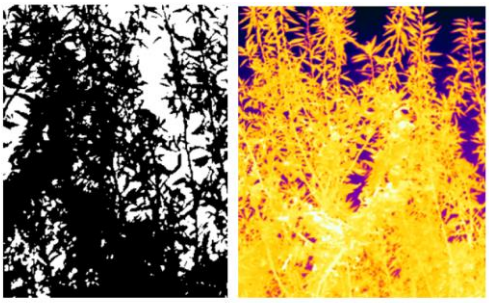

Figure 2. Example of image processing using the software developed by García-Tejero et al (2012). On the right, the initial thermal imaging; on the left, a bitmap image, in which the black area represents the pixels of the thermal image considered to calculate the canopy temperature.

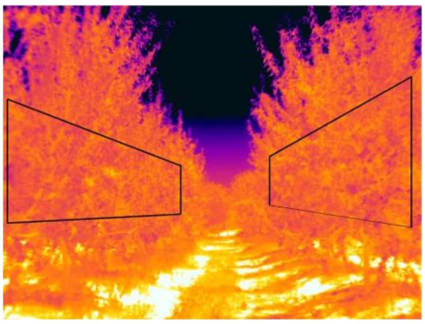

Figure 3. Example of image processing at row level using the ThermaCam Research Pro (Flir Systems, USA).

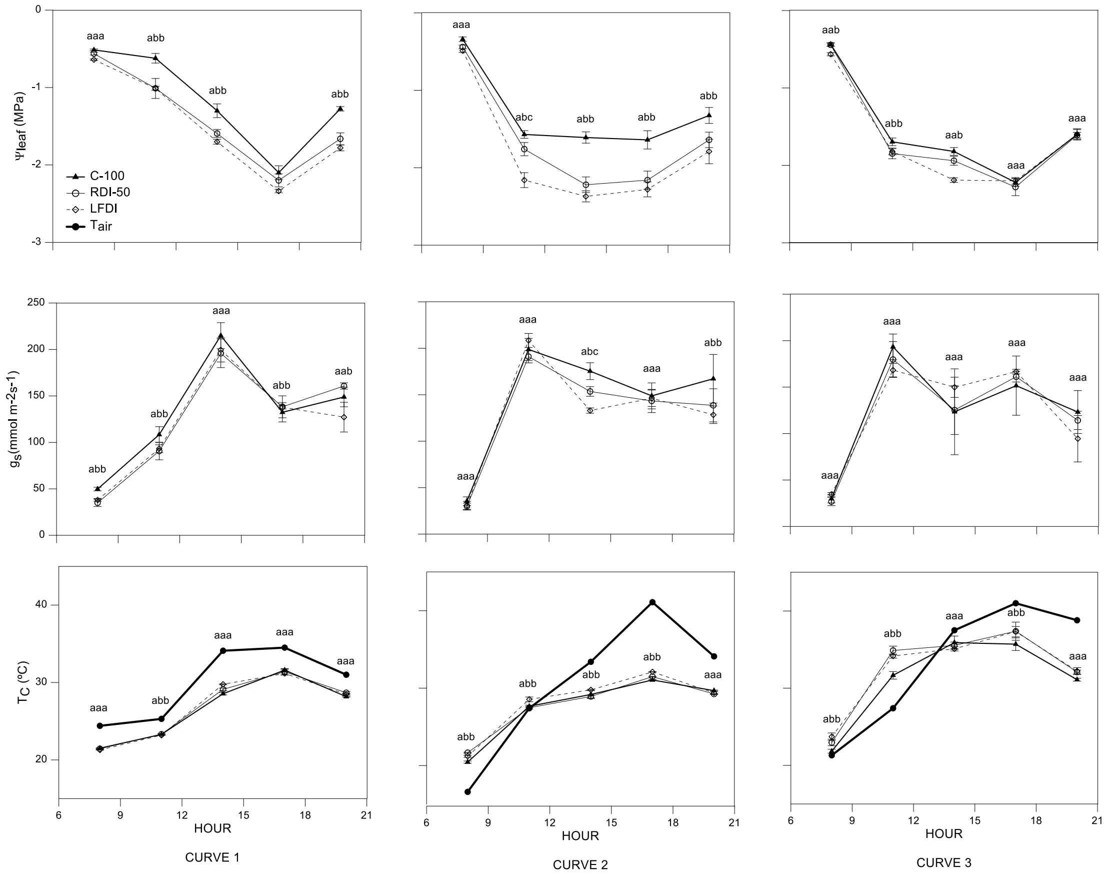

Figure 4. Daily curves of leaf water potential (Ψ_{leaf}), stomatal conductance (g_s) canopy temperature (T_c) and air temperature (T_{air}) in almond trees subjected to different irrigation doses: C-100, full irrigated treatment; RDI-50, regulated deficit irrigation; LFDI, low-frequency deficit irrigation. Letters a, b, and c show significant differences between C-100, RDI-50 and LFDI treatments, respectively ($p<0.05$).

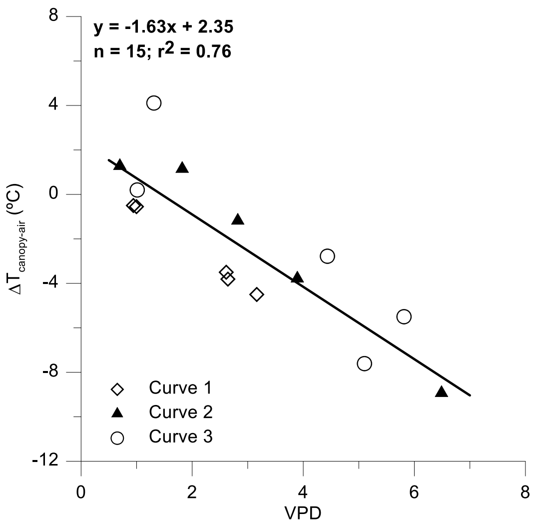

Figure 5. Non-water stress baseline ($\Delta T_{canopy\text{-}air}$) = a*VPD + b. Data obtained for the DOYs 210, 217 and 239 and using the readings taken at 8:30, 11:30, 14:30, 15:30 and 20:00.

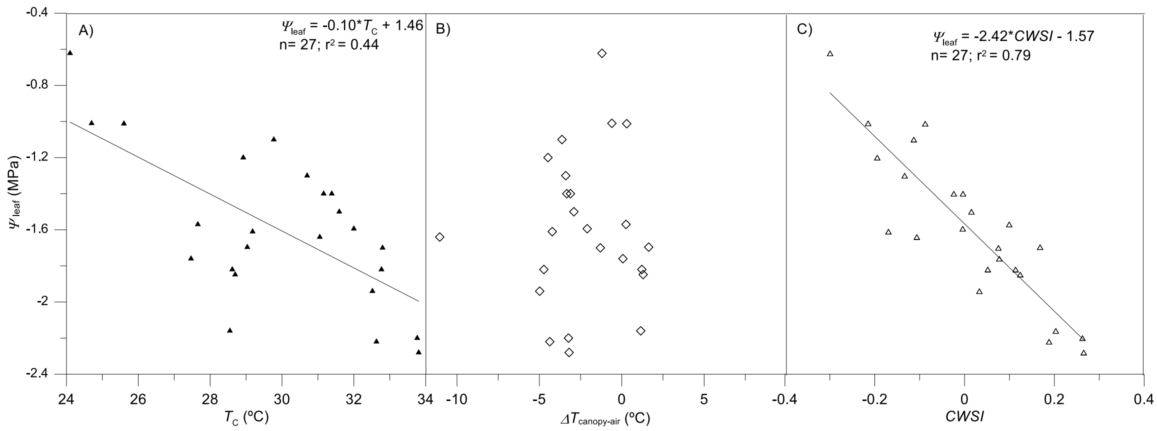

Figure 6. Relationships between canopy temperature readings (*T*C), the difference between canopy and air temperature (*ΔT*canopy-air) and crop water stress index (*CWSI*) with leaf-water potential (*Ψ*leaf).

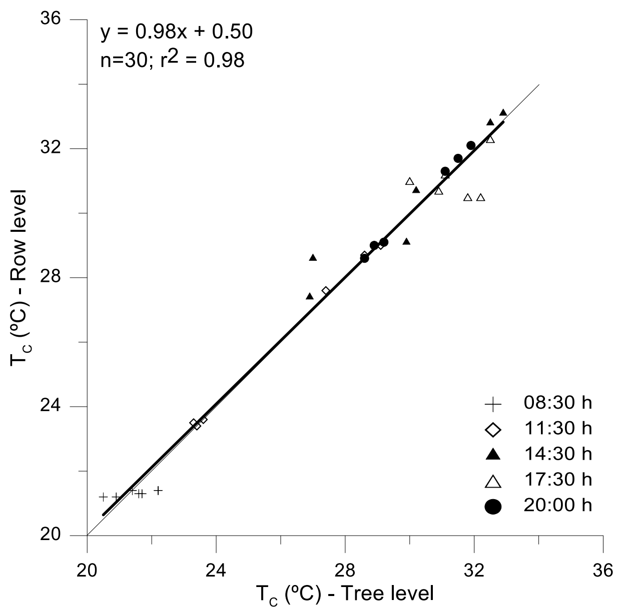

Figure 7. Relationships between canopy temperature readings (*T*C) at tree and row level.

TABLES

Table 1. Climatic conditions, water requirements and irrigation doses applied during the season

Period (DOY)	T_{air} (ºC)	*RH* (%)	**Rainfall** (mm)	ET_0 (mm)	K_C	ET_C (mm)	**C-100** (mm)	**RDI-50** (mm)	**LFDI** (mm)
60 to 90	13.53	70.18	55.6	92.11	0.3	27.63	0	0	0
91 to 120	17.95	72.96	35.6	114.84	0.55	34.74	8.03	8.03	8.031
121 to 151	21.42	54.06	12.6	175.79	0.9	118.66	109.21	109.21	109.21
152 to 181	23.40	58.88	7.4	176.94	1.05	167.21	161.66	108.32	107.88
182 to 212	25.24	58.81	0.2	184.24	1.15	190.69	190.54	91.46	77.85
213 to 243	26.05	54.06	0	173.82	1.15	179.90	179.90	88.15	79.56
244 to 273	22.66	78.06	175.8	104.99	0.8	75.59	23.02	23.02	23.02
274 to 304	19.93	77.67	73.2	79.86	0.7	50.31	12.5	12.5	12.5

DOY. day of the year; T_{air}. average air temperature; RH. average relative humidity. ET_0. reference evapotranspiration; K_C. crop coefficient; ET_C. crop evapotranspiration; C-100. control treatment; SDI-50. regulated deficit irrigation at 50% of ET_C during the kernel filling period; LFDI. low-frequency deficit irrigation during the kernel filling period.

Table 2. Average values of air temperature (T_{air}). relative humidity (RH) and vapour pressure deficit (VPD) registered during the daily curves

	Curve 1 (210 DOY)			Curve 2 (217 DOY)			Curve 3 (239 DOY)		
Hour	T_{air} (ºC)	RH (%)	VPD (kPa)	T_{air} (ºC)	RH (%)	VPD (kPa)	T_{air} (ºC)	RH (%)	VPD (kPa)
08:30	24.4	63	0.94	16.6	63	0.70	21.3	60	1.01
11:30	25.3	69	0.99	27.4	50	1.82	27.4	64	1.31
14:30	34.1	51	2.61	33.4	45	2.82	37.5	31	4.43
17:30	34.5	42	2.29	42.1	21	6.49	41.0	25	5.81
20:00	31	41	1.84	34.1	27	3.90	38.8	26	5.10

T_{air}. average air temperature; RH. average relative humidity; VPD. vapour pressure deficit

Table 3. Pearson's correlation coefficients between thermal information and the studied physiological variables

Hour		T_C	$\Delta T_{canopy\text{-}air}$	*CWSI*	I_G
8:30	g_s	-0.32*	ns	-0.40*	ns
	Ψ_{leaf}	ns	ns	ns	ns
11:30	g_s	ns	ns	ns	ns
	Ψ_{leaf}	-0.85**	-0.69*	-0.85**	ns
14:30	g_s	-0.70*	ns	-0.82**	ns
	Ψ_{leaf}	-0.39*	ns	-0.69*	ns
17:30	g_s	ns	-0.70*	-0.62*	ns
	Ψ_{leaf}	-0.39*	ns	-0.34*	0.74**
20:00	g_s	-0.75*	ns	ns	ns
	Ψ_{leaf}	ns	ns	ns	ns

T_C. canopy temperature; $\Delta T_{canopy\text{-}air}$. difference between canopy and air temperature; *CWSI*. crop-water stress index; I_G. relative index of stomatal conductance; g_s. stomatal conductance to water vapour; Ψ_{leaf}. leaf-water potential in shaded leaves. * and ** show significant relationships at confidence level of 95 and 99%. respectively.

Table 4. Example of false-coloured images taken at tree and row level during the Curve 1 in the different irrigation treatments and moment of the day. The values of canopy temperature (T_C) correspond to the average of five measurements taken for each treatment and moment of the day.

	Tree level			Row level		
	C-100	**RDI-50**	**LFDI**	**C-100**	**RDI-50**	**LFDI**
08:30	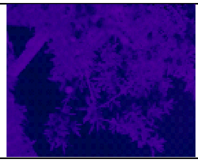	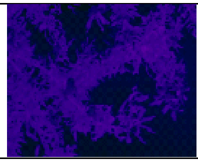	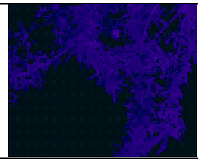	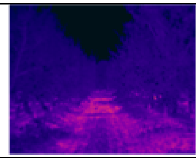	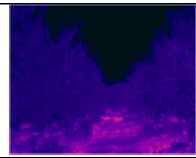	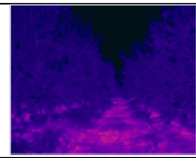
T_C (ºC)	21.7	21.6	21.4	21.3	21.3	21.4
11:30	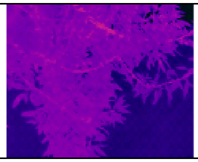	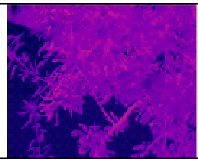	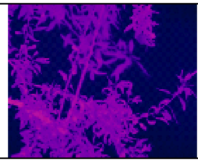	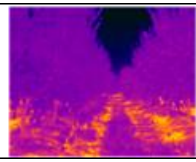	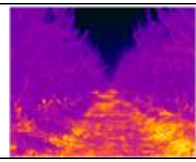	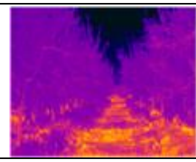
T_C (ºC)	23.3	23.6	23.4	23.5	23.6	23.4
14:30	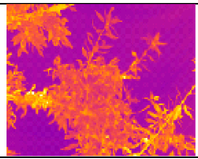	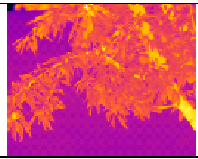	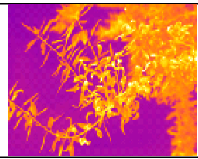	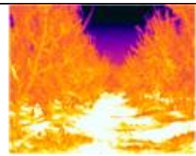	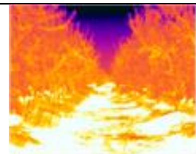	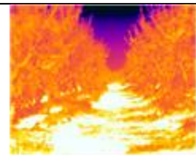
T_C (ºC)	26.9	27.0	29.9	27.4	28.6	29.1
17:30	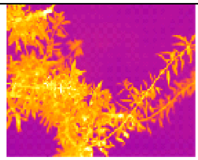	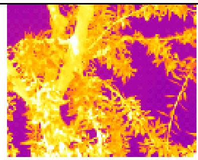	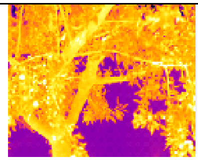	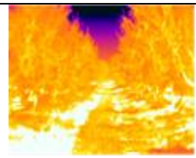	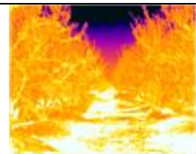	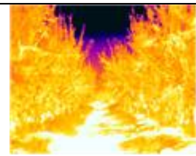
T_C (ºC)	32.5	30.9	30.0	32.3	30.7	31.0
20:00	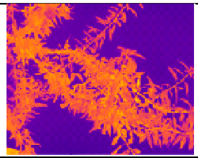	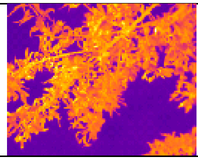	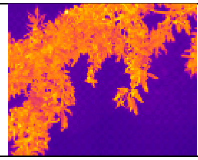	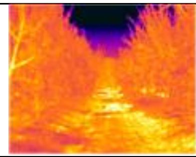	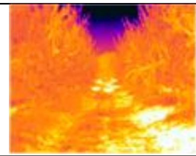	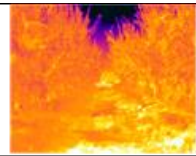
T_C (ºC)	29.2	28.6	28.9	29.1	28.6	29.0

Table 5. Example of false-coloured images taken at tree and row level during the Curve 2 in the different irrigation treatments and moment of the day. The values of canopy temperature (T_C) correspond to the average of five measurements taken for each treatment and moment of the day.

	Tree level			Row level		
	C-100	**RDI-50**	**LFDI**	**C-100**	**RDI-50**	**LFDI**
08:30	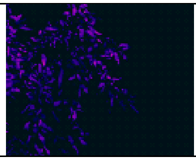	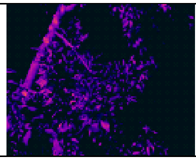	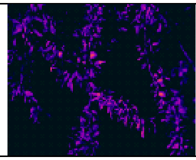	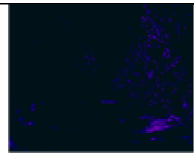	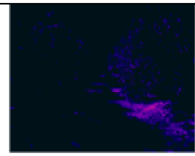	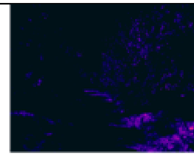
T_C (ºC)	20.9	20.5	22.2	21.2	21.2	21.4
11:30	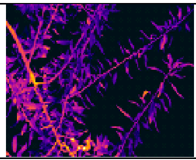	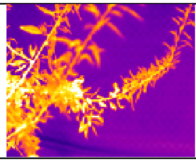	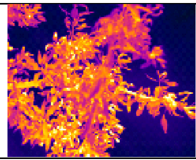	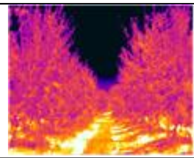	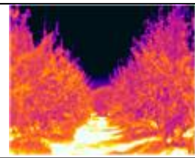	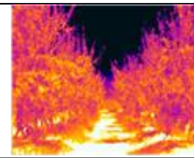
T_C (ºC)	27.4	28.6	29.1	27.6	28.7	29.0
14:30	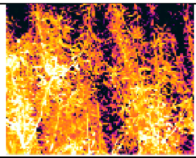	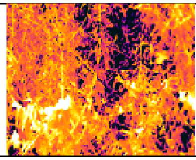	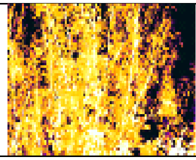	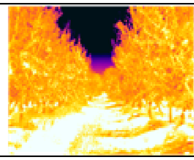	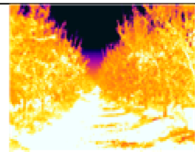	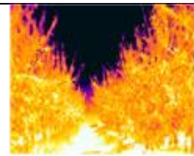
T_C (ºC)	30.2	32.5	32.9	30.7	32.8	33.1
17:30	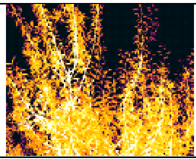	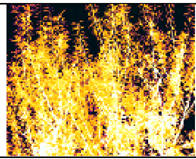	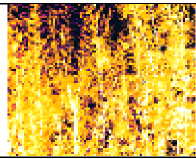	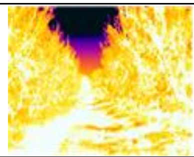	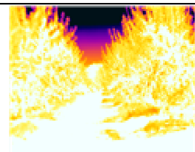	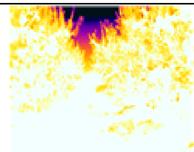
T_C (ºC)	31.8	32.2	31.1	30.5	30.5	31.2
20:00	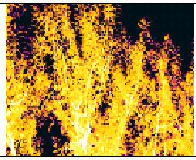	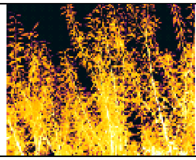	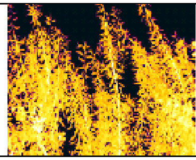	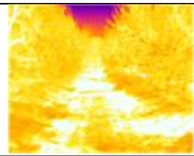	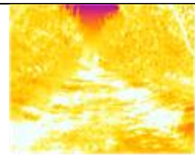	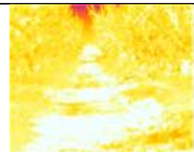
T_C (ºC)	31.1	31.5	31.9	31.3	31.7	32.2